Journal of Pharmaceutical Analysis 11 (2021) 183–190

Contents lists available at ScienceDirect

Journal of Pharmaceutical Analysis

journal homepage: www.elsevier.com/locate/jpa

Original article

A dual-signal sensor for the analysis of parathion-methyl using silver nanoparticles modified with graphitic carbon nitride

Yuan Li [a], Mengqi Wan [a], Guosheng Yan [a], Ping Qiu [a, b, *], Xiaolei Wang [c]

[a] Department of Chemistry, Nanchang University, Nanchang, 330031, China
[b] Jiangxi Province Key Laboratory of Modern Analytical Science, Nanchang University, Nanchang, 330031, China
[c] Institute of Translational Medicine, Nanchang University, Nanchang, 330088, China

ARTICLE INFO

Article history:
Received 26 November 2019
Received in revised form
21 April 2020
Accepted 21 April 2020
Available online 26 April 2020

Keywords:
Organophosphorus pesticides
Dual-signal
g-C_3N_4/AgNPs
Fluorescence
UV–vis spectrophotometry

ABSTRACT

A highly sensitive and selective method was developed for both UV–vis spectrophotometric and fluorimetric determination of organophosphorus pesticides (OPs). This method used silver nanoparticles (AgNPs) modified with graphitic carbon nitride (g-C_3N_4). The AgNPs reduced the fluorescence intensity of g-C_3N_4. Acetylthiocholine (ATCh) could be catalytically hydrolyzed by acetylcholinesterase (AChE) to form thiocholine, which induces aggregation of the AgNPs. This aggregation led to the recovery of the blue fluorescence of g-C_3N_4, with excitation/emission peaks at 310/460 nm. This fluorescence intensity could be reduced again in the presence of OPs because of the inhibitory effect of OPs on the activity of AChE. The degree of reduction was found to be proportional to the concentration of OPs, and the limit of fluorometric detection was 0.0324 μg/L (S/N = 3). In addition, the absorption of the g-C_3N_4/AgNPs at 390 nm decreased because of the aggregation of the AgNPs, but was recovered in presence of OPs because of the inhibition of enzyme activity by OPs. This method was successfully applied to the analysis of parathion-methyl in real samples.

1. Introduction

The widespread and long-term use of pesticides has caused serious pollution of agricultural products and the environment, and ultimately endangers ecosystems and human life [1,2].The development of organophosphorus pesticides (OPs) has been rapid since their entry into the market in 1943 because these compounds decompose easily and have a short residual time [3]. However, OPs have residual problems, and some varieties cause acute toxicity and delayed neurotoxicity. Since the 1970s, the rate of the research and development of OPs has slowed down considerably. In China, OPs account for 70% of the total pesticides. Excessive or improper application of pesticides is a main cause of food contamination. Acetylcholinesterase (AChE) degrades acetylcholine and also can stop the excitatory effects of neurotransmitters on the postsynaptic membrane and ensure the normal transmission of neural signals in the body, so AChE plays a key role in the biological nerve conduction between cholinergic synapses [4]. OPs inhibit the activity of AChE in living organisms, leading to metabolic disorders of acetylcholine, delayed neurotoxicity, movement disorders, coma, paralysis of the respiratory center, and even death [5–7] (see Scheme 1).

In recent years, methods using conventional techniques, such as gas chromatography [8], liquid chromatography [9,10], enzyme inhibition methods [5], immunoassays [11–13], and molecularly imprinted polymer (MIP) sensors [14,15], have been developed to detect OPs. Although these methods are effective for the analysis of OPs, there are still some disadvantages, including requiring time-consuming pretreatment of samples, expensive equipment, and skilled operators. In addition, onsite detection can also be easily affected by external conditions, including instruments and environment.

Currently, optical biosensors are being developed rapidly [16], and there are many fluorescent sensors now available based on various kinds of nanoparticles, such as upconversion nanoparticles [17,18], non-metallic and metallic quantum dots [19–21], organic dyes [22], and sensors to detect OPs. Bioconjugates based on quantum dot preparations have been developed that can specifically detect diazinon [23], and fluorescence sensors based on boron nitride quantum

Peer review under responsibility of Xi'an Jiaotong University.
* Corresponding author. Department of Chemistry, Nanchang University, Nanchang, 330031, China.
E-mail address: pingqiu@ncu.edu.cn (P. Qiu).

https://doi.org/10.1016/j.jpha.2020.04.007

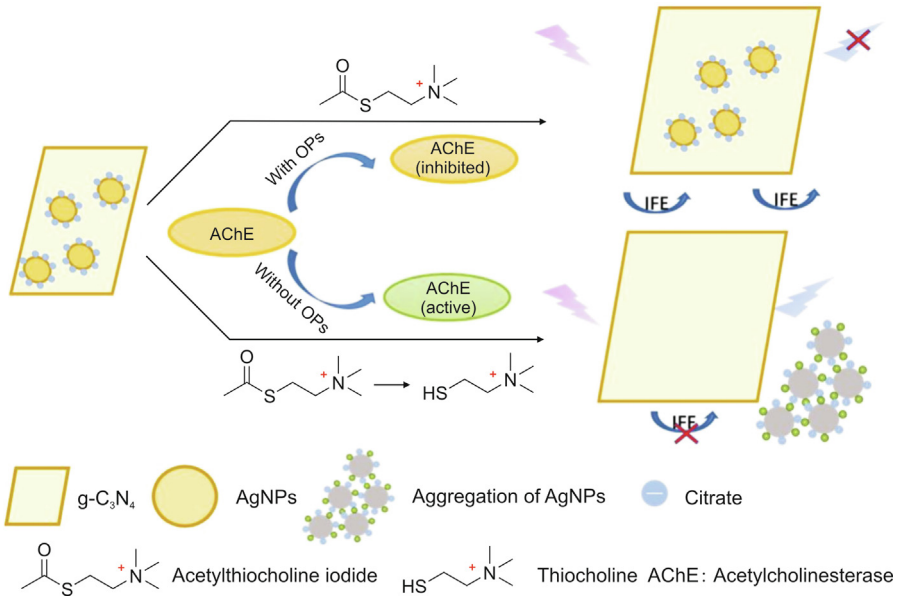

Scheme 1. Mechanism of detecting organophosphorus pesticides based on g-C_3N_4/AgNPs. IFE: inner filter effect; AChE: acetylcholinesterase.

dots and gold nanoparticles have been developed that enable the ultrasensitive detection of AChE activity [24]. However, these methods require material that takes a long time to synthesize or is formed from a low yielding reaction, which is not suitable for rapid detection. In the present study, the fluorescence of g-C_3N_4 was used to construct a method using a combination of ultraviolet and fluorescent double signals to quantitatively analyze OPs.

g-C_3N_4, an important polymer semiconductor material, has excellent chemical stability and is environmentally friendly, and has attracted great attention from researchers in recent years [25]. g-C_3N_4 is a carbon-based material with a high fluorescence quantum yield [26,27], which can be produced by the direct pyrolysis of carbon-containing and nitrogen-containing organic precursors, such as urea [28], ammonium thiocyanate [29], and melamine [30] in a semi-closed system. Importantly, g-C_3N_4 is the most stable allotrope of carbon nitride and is also a light-stable substance. There have been many reports on pesticide residue analysis using methods based on g-C_3N_4. Zhang et al. [31] prepared zinc oxide (ZnO) hybridized with graphite-like C_3N_4 (ZnO/g-C_3N_4) nanoflowers for gas chromatography–mass spectroscopy, which was successfully used for the simultaneous determination of nine pesticide residues in real samples, with satisfactory recoveries of 79.1%–103.5%. Yin et al. [32] proposed a photoelectrochemical (PEC) biosensor based on g-C_3N_4 and CdS quantum dots, which might provide useful information on the carcinogenic mechanisms of pesticides.

In our work, a dual-signal parathion-methyl nanoprobe, combining fluorescence with UV–vis spectrophotometry, was developed to analyze OPs based on g-C_3N_4 modified AgNPs. AgNPs, as fluorescent absorbers, can effectively inhibit the fluorescence of g-C_3N_4 by the inner filter effect (IFE), which results in a decrease of fluorescence. AChE can hydrolyze acetylcholine to form thiocholine (TCh), and the HS groups on TCh can then combine with the AgNPs, causing aggregation of the AgNPs and restoring the fluorescence intensity of g-C_3N_4. Because of the aggregation of the AgNPs, the absorbance of g-C_3N_4/AgNPs at 390 nm is decreased from the value for free g-C_3N_4. However, when OPs are present in the system, the absorbance will be recovered because of the enzyme inhibition of the OPs. Based on this mechanism, a highly sensitive and selective dual-signaling method for detecting parathion-methyl (PM) was established. This detection system can be used to measure PM in vegetable and water samples.

2. Experimental

2.1. Reagents and apparatus

PM was provided by Chem Service (West Chester, PA, USA). Various concentrations were prepared by serial dilution of a stock solution of PM (10 μg/L in methanol). Acetylthiocholine iodide (ATCh) and AChE (1323 unit/mg) were purchased from Sigma-Aldrich (St. Louis, MO, USA). ATCh (20 mM) solution was newly prepared in dual-distilled water and the service time was less than 3 h. AChE (1 unit/mL) was dissolved with Tris-HCl buffer (pH 7.5, 0.02 nM). Silver nitrate ($AgNO_3$), sodium borohydride ($NaBH_4$, 96%), and sodium citrate ($C_6H_5O_7Na_3 \cdot 2H_2O$) were purchased from Sinopharm Chemical Reagent Co., Ltd. (Shanghai, China). Melamine was obtained from Aladdin Ltd. (China). All chemicals were analytical grade reagents, all of which were prepared using double distilled deionized water. All glassware was washed three times with aqua regia and double-distilled water.

2.2. Instrumentation

Zeta potentials were obtained using a Nano ZS90 (Malvern, UK). The fluorescence spectra were performed on an F-4600 fluorescence spectrometer (Hitachi, Japan). The phosphorescence lifetimes were recorded on a FluoroMax-4 luminescence spectrometer (Horiba, USA). The UV spectra were recorded by using UV-2450 Shimadzu Vis-spectrometer (Hitachi, Japan). Transmission electron microscopy (TEM) measurements were taken on JEM-2100 (Japan) and the operational accelerating voltage was at 200 kV. The correlation point and linear resolutions were 0.23 nm and 0.14 nm, respectively. A drop of solution on a carbon-coated copper grid to prepare samples of TEM characterized was dried at room temperature.

2.3. Preparation of g-C_3N_4

g-C_3N_4 was synthesized by the direct thermal treatment of melamine as reported in previous work [30]. Melamine (10 g) was placed in an alumina crucible with a cover and then heated to 600 °C with a heating rate of 3 °C/min under air conditions, and then kept at that temperature for 2 h. After cooling the product to room temperature, yellow g-C_3N_4 powder was obtained. The product was taken out and ground into fine powder using ultrasound treatment of the bulk g-C_3N_4 in water for approximately 20 h [33].

2.4. Preparation of AgNPs

According to a literature procedure [34], a 250 mL flat-bottomed flask containing 100 mL of secondary distilled water was placed in an ice-water bath (5 °C). Then, $AgNO_3$ (250 μL, 100 mM), BH_4Na (6 mL, 5 mM), and sodium citrate solution (250 μL, 100 mM) were added to the flask with rapid stirring. The formation of AgNPs could be preliminarily determined when the color of the solution changed from colorless to light yellow. The reaction was continued for 30 min and the product was placed under dark conditions for 24 h until further use.

2.5. Fluorometric detection of PM

Briefly, a series of different concentrations (10 μL) of PM and AChE (5 μL, 1.0 U/mL) were incubated in $NaCO_3$–$NaHCO_3$ (45 μL, 10 mol/L, pH 9.0) at 37 °C for 20 min. Next, ATCh (5 μL, 1.0 mol/L) was added and the mixture was incubated at 37 °C for 30 min. Finally, g-C_3N_4 (200 μL, 3.0 mg/mL) and AgNPs (235 μL, 8.5 nmol/L) were added and the resulting solution was made up to 500 μL with $NaCO_3$–$NaHCO_3$ (10 mmol/L, pH 9.0). The fluorescence emission spectrum was measured and the fluorescence intensity at 460 nm was recorded.

2.6. UV–vis spectrophotometric detection of PM

To assess the possibility of a dual-read assay for OPs, a series of different concentrations of PM (10 μL) was added to AChE (6 μL, 1.0 U/mL) in $NaCO_3$–$NaHCO_3$ (138 μL, 10 mM, pH 10.0) and incubated for 20 min at 37 °C. Then, ATCh (6 μL, 1.0 mmol/L) was added and the solution was made up to 600 μL with $NaCO_3$–$NaHCO_3$, and left for 30 min. Finally, g-C_3N_4 (240 μL, 3.0 mg/mL) and AgNPs (200 μL, 8.5 nmol/L) were added sequentially. The UV–vis absorption spectrum was measured and the absorption spectrum at 390 nm was recorded.

2.7. Detection of PM in real samples

The application of g-C_3N_4/AgNPs for the analytical detection of PM in real samples was investigated in water and vegetable samples. Water samples were obtained from Runxi Lake in Nanchang University, Nanchang, Jiangxi Province, China, and food samples were bought from the local market of Nanchang city, Jiangxi Province, China. The pretreatment of these samples was based on methods in previous literature reports [35]. First, the samples were spiked with a series of concentrations of PM and kept for 24 h. To remove the insoluble matrix, the spiked solution was filtered using a FES membrane (0.22 μm). Equal volumes of the filtrate and $NaCO_3$–$NaHCO_3$ (10 mM, pH 9.0) were mixed and the fluorescence emission and UV absorption spectra of the samples were recorded.

3. Results and discussion

3.1. Characterization of g-C_3N_4 and AgNPs

In this study, AgNPs were used as a fluorophore/absorber pair because their extinction coefficient is 100 times higher than that of gold nanoparticles [36,37]. Fig. 1A shows the fluorescence emission spectra of g-C_3N_4 and the UV–vis absorption spectra of the AgNPs. It can be seen that there was a strong overlap between the emission spectrum and the absorption spectrum, which provided the necessary condition for the inner filter effect (IFE) [38]. IFE refers to the phenomenon that the fluorescence decreases due to the

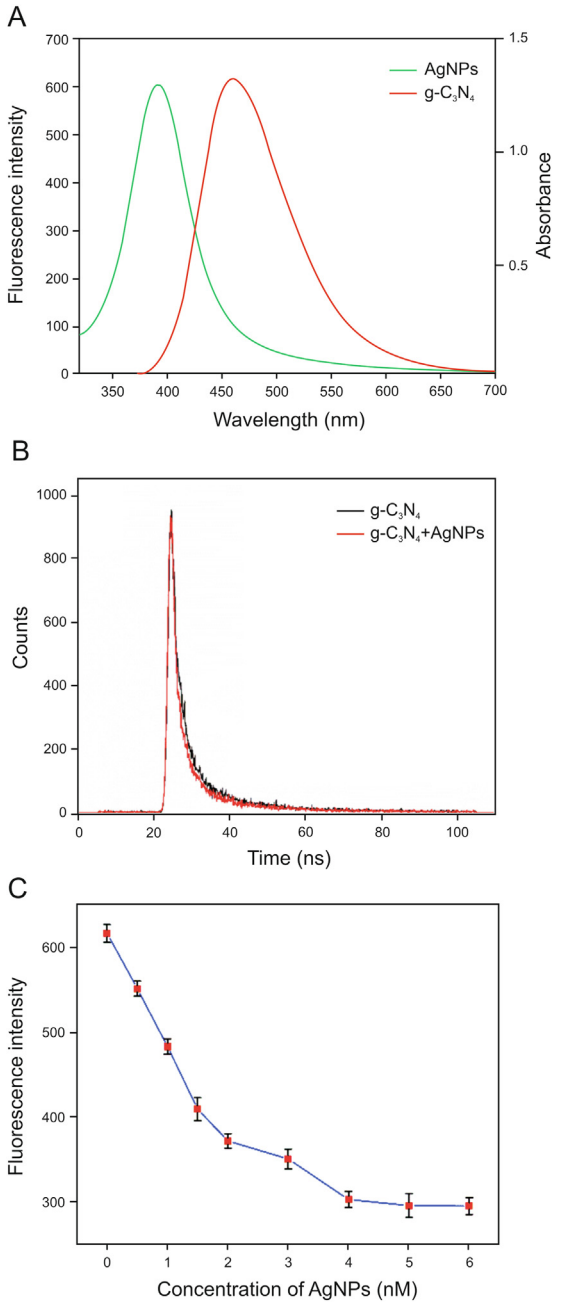

Fig. 1. (A) The fluorescence spectra of g-C_3N_4 and the absorption spectra of AgNPs. (B) The fluorescence lifetimes of g-C_3N_4 in presence of AgNPs and g-C_3N_4 in absence of AgNPs. (C) The influence of concentration of AgNPs on fluorescence intensity of g-C_3N_4.

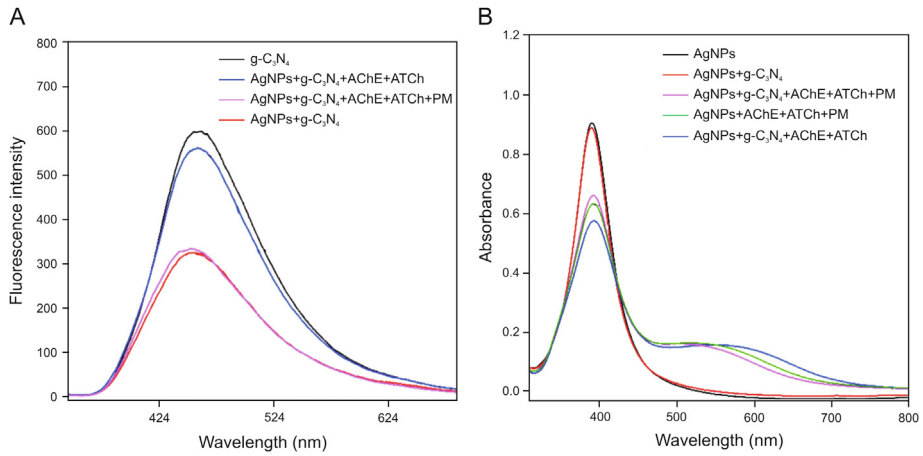

Fig. 2. (A) The fluorescence emission spectrum of g-C_3N_4 interacting with different substrates. (B)The absorption spectra of g-C_3N_4, AgNPs and the mixture with different substrates.

absorption of excitation light or emission light by the phosphor or other light-absorbing substances when the concentration of the phosphor is large or coexists with other light-absorbing substances. The AgNPs prepared by the sodium citrate reduction method were easily absorbed by citrate anions, and the electrostatic repulsion between the AgNPs kept them stable without polymerization. Moreover, it was further supported by the zeta potential value of the AgNPs of −26.4 mV, which was consistent with the literature value of the zeta potential of g-C_3N_4 for −28.9 mV [38]. Therefore, there was no electrostatic attraction between the AgNPs and g-C_3N_4 because both the AgNPs and g-C_3N_4 are negatively charged. In general, the fluorescence lifetime is largely unaffected by the fluorescence intensity. However, if a high-efficiency fluorescence resonance energy transfer (FRET) process is employed, the fluorescence lifetime will change substantially. As shown in Fig. 1B, the average fluorescence lifetime of g-C_3N_4 did not change appreciably in the presence of the AgNPs, indicating that energy transfer did not occur between g-C_3N_4 and AgNPs. Fig. 1C shows that the fluorescence intensity of g-C_3N_4 decreased gradually as the concentration of the AgNPs increased from 0 to 6 nM. When the concentration of the AgNPs reached 4 nM, the maximum reduction in fluorescent intensity was obtained. Therefore, we believe that the decrease in the fluorescence intensity of g-C_3N_4 was because of the IFE rather than FRET, and a 4 nM concentration of AgNPs was used in subsequent experiments.

3.2. Mechanism of the dual-signaling determination of PM

It is well known that g-C_3N_4 has strong fluorescence photostability and solubility. Fig. 2A shows a comparison of the fluorescence emission spectra of g-C_3N_4 after interaction with different substrates. It is obvious that g-C_3N_4 has strong fluorescence intensity. When the AgNPs were added, the fluorescence intensity decreased, which is because of the IFE of the AgNPs as mentioned above [39]. The IFE does not require intermolecular interactions between the absorber and the fluorophore, unlike some widely used conventional sensing mechanisms, such as FRET, thus providing a simple alternative fluorescent nanoprobe [40]. AgNPs are effective absorbers in IFE systems because AgNPs have broad absorption bands and a high extinction coefficient in the visible and UV−visible regions [41].

When AChE and ATCh were added to g-C_3N_4/AgNPs, we found that the fluorescence was recovered. This recovery occurred because ATCh was catalyzed by AChE to produce TCh, and then Ag−S bonds between TCh and the AgNPs were formed, resulting in aggregation of the AgNPs. However, once PM was added to the mixture, the fluorescence of g-C_3N_4/AgNPs was reduced because of the inhibitory effect of PM on AChE. According to this detection mechanism, we designed a g-C_3N_4/AgNPs/AChE fluorescent probe to detect OPs.

A similar mechanism can be used to detect PM using UV−Vis spectrophotometry based on g-C_3N_4/AgNPs. Fig. 2B shows the absorption spectra of the AgNPs, g-C_3N_4, and mixtures of AgNPs and g-C_3N_4 with different substrates. The AgNPs had a strong absorption peak at 390 nm and there was no change in the peak shape after addition of g-C_3N_4. Addition of AChE and ATCh to the g-C_3N_4/AgNPs resulted in a sharp drop in absorbance, caused by aggregation of the AgNPs. The absorbance was recovered again when PM was mixed with the solution because of the inhibitory effect of PM on AChE. Interestingly, the absorbance of the solution with g-C_3N_4 was stronger than that without g-C_3N_4. Therefore, spectrophotometry based on g-C_3N_4/AgNPs can provide sensitivity high

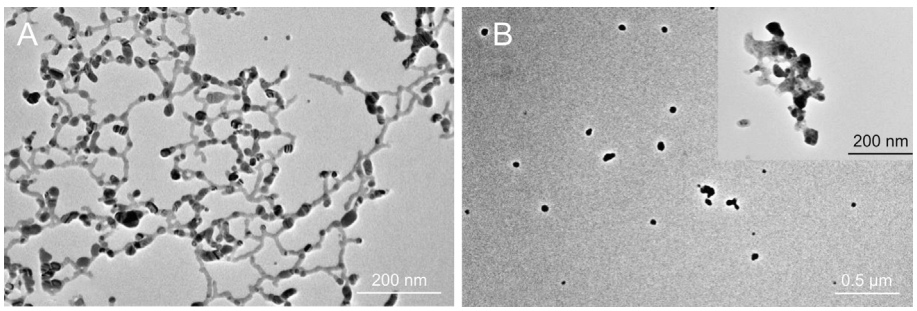

Fig. 3. The TEM images of (A) g-C_3N_4/AgNPs, and (B) AChE and ATCh existing in g-C_3N_4/AgNPs. Inset: The TEM image of the aggregation state of AgNPs.

enough for the detection of OPs.

The aggregation behavior of AgNPs in the g-C_3N_4 solution, promoted by TCh generated by the addition of AChE and ATCh, was verified by TEM images. Fig. 3A shows a TEM photograph of the dispersion of the AgNPs in a g-C_3N_4 solution. It can be seen that the AgNPs had uniform, spherical, and monodisperse shapes, which were well dispersed in the g-C_3N_4 skeletons. However, as can be seen from Fig. 3B, the AgNPs were highly aggregated after addition of AChE and ATCh. Together with the spectral results, these TEM observations confirm our theory of the detection mechanism.

3.3. Optimization of the detection conditions for fluorescence analysis

To obtain the optimal sensing response for the detection of PM using g-C_3N_4/AgNPs for fluorescence analysis, the experimental parameters affecting sensitivity and selectivity were all optimized, including the concentration of g-C_3N_4 and the AgNPs, the pH, and the reaction time.

The optimum values of the reaction parameters could be determined by the reduction efficiency, which was defined as $(F_0-F)/F_0$ (where F_0 and F are the fluorescence intensity of g-C_3N_4 in the presence and absence of the AgNPs, respectively). As the optimal concentration of the AgNPs was previously determined to be 4 nM, the influence of the concentration of g-C_3N_4 was studied. From Fig. 4A, it can be clearly observed that the efficiency of the reduction in fluorescence intensity reached its maximum when the concentration of g-C_3N_4 was 1.2 mg/mL. Therefore, a g-C_3N_4 concentration of 1.2 mg/mL was used in further experiments. Then, the influence of pH on the experiment was investigated over a range of pH 5–12. As shown in Fig. 4B, the reduction in the fluorescence intensity of g-C_3N_4/AgNPs reached a maximum at pH 9.0. The reaction time of the fluorescence recovery of g-C_3N_4/AgNPs also had an influence on the response of the nanoprobe. We explored the efficiency of the reduction in fluorescence intensity while varying the reaction time from 0 to 18 min (Fig. 4C). The fluorescence intensity of the mixed solution was recorded every 3 min at an excitation wavelength of 310 nm. When the time was longer than 12 min, the fluorescence intensity reached a plateau as the reaction reached completeness. Therefore, 12 min was used as the measurement time in subsequent experiments.

3.4. Optimization of the detection conditions for UV–vis analysis

Similarly, we also optimized the experimental conditions for the UV analysis, as shown in Fig. 5. The absorption spectra of g-C_3N_4/AgNPs in ATCh solution reached a maximum at pH 10 (Fig. 5A). Because the concentration of ATCh affects the aggregation state of the AgNPs, four different concentrations of ATCh were investigated using reaction time from 0 to 40 min (Fig. 5B). It was found that 10 μM of ATCh had little effect on the AgNPs, but excessive concentrations of ATCh reduced the absorbance, which may be a result of electrostatic interactions between the positively charged ATCh and negatively charged AgNP molecules leading to aggregation of the AgNPs.

3.5. Specificity of the g-C_3N_4/AgNPs nanoprobe

To estimate the selectivity of the established method, several potential interferents in water and vegetables were examined. Fig. 6 shows the changes in fluorescence intensity and absorbance of the interferents added to the g-C_3N_4/AgNPs system, with PM (0.5 μg/L) as a blank group. It was found that the interferents had little effect on the fluorescence intensity and absorbance of g-C_3N_4/AgNPs. These results demonstrated that the nanoprobe had a specific response to PM, regardless of the presence of an interferent. The repeatability of the g-C_3N_4/AgNPs system was also assessed and the relative standard deviation ($n = 3$) was determined to be less than 4.5%. To analyze the stability, samples containing a PM concentration of 0.5 μg/L were stored in the refrigerator at 4 °C. After 15 days, the fluorescence intensity was measured and the standard deviation was <2.3%. These results confirmed that g-C_3N_4/AgNPs system was stable and the nanoprobe process had good repeatability.

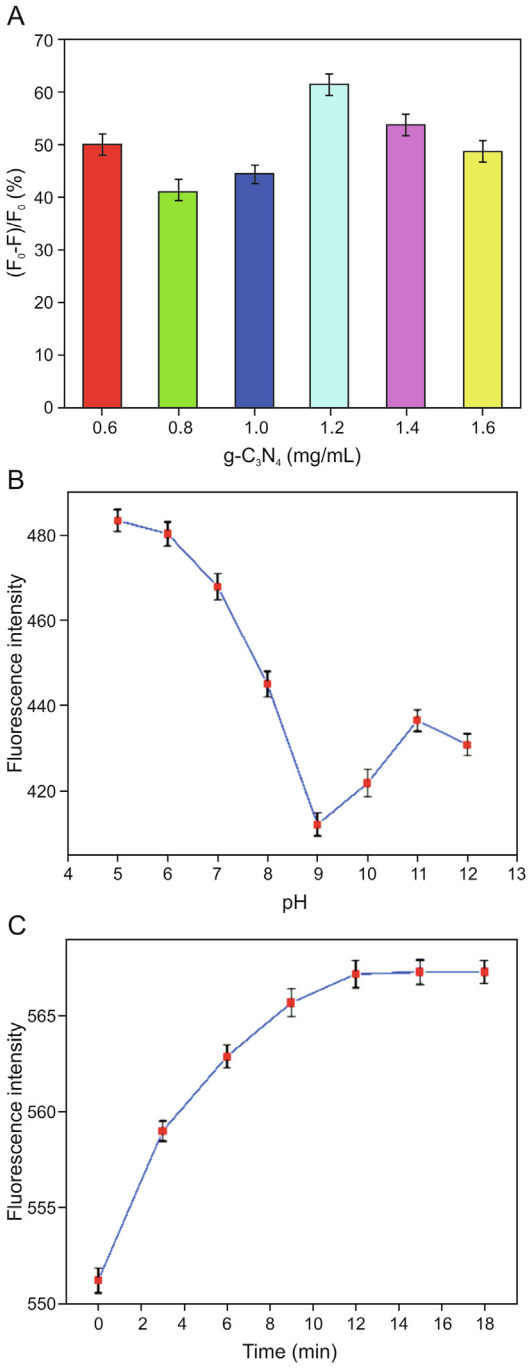

Fig. 4. (A) The reduction efficiency of fluorescence intensity of different concentrations of g-C_3N_4 in the presence of AgNPs. (B) The fluorescence intensity of g-C_3N_4/AgNPs under different pH. (C) The influence of the reaction time of the fluorescence recovery of g-C_3N_4/AgNPs.

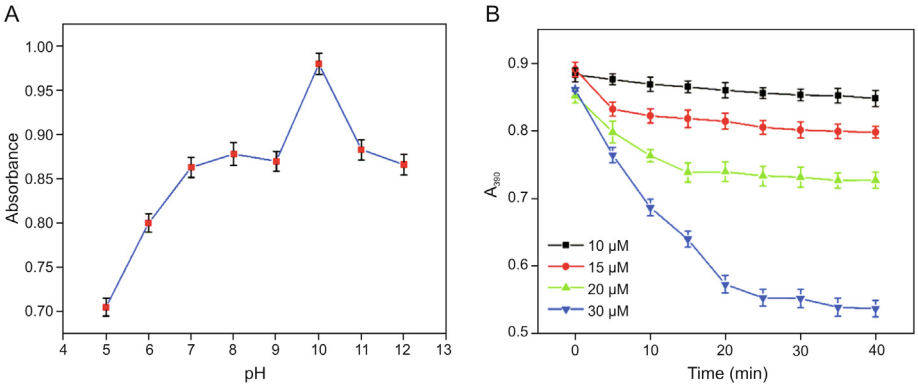

Fig. 5. (A) The influence of pH on the absorbance of g-C_3N_4/AgNPs in ATCh solution. (B) Variation of absorption versus the reaction time for AgNPs with different concentrations of ATCh.

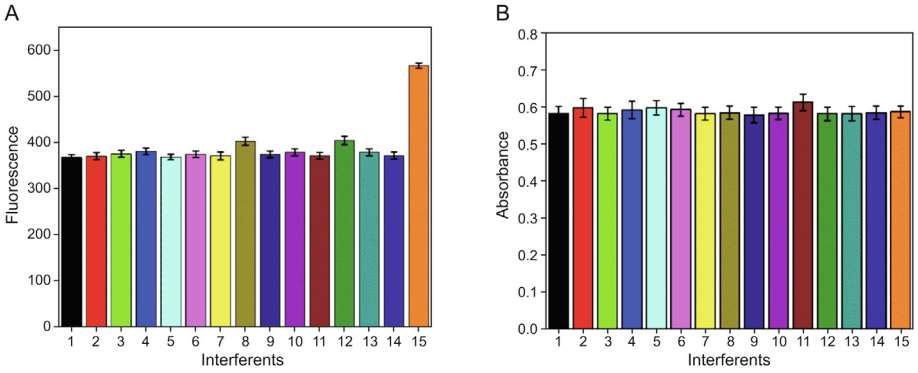

Fig. 6. The specificity of g-C_3N_4/AgNPs solution with different interferents (1: Cu^{2+}, 2: Fe^{3+}, 3: Fe^{2+}, 4: Al^{3+}, 5: Mn^{2+}, 6: Ca^{2+}, 7: Na^{+}, 8: Mg^{2+}, 9: K^{+}, 10: PO_4^{3-}, 11: HPO_4^{2-}, 12: NO_3^{-}, 13: Vc, 14: VB_2, 15: PM). (A) Fluorescence, and (B) UV–vis spectrophotometry.

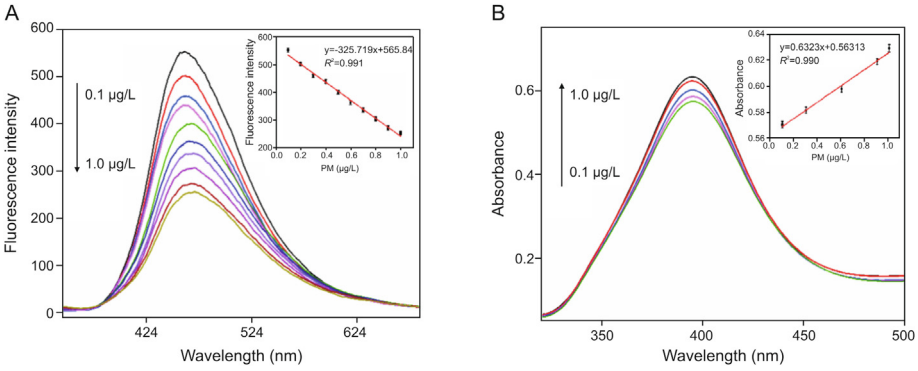

Fig. 7. Response to PM at increasing concentrations and the linear calibration plot for PM. (A) Fluorescence, and (B) UV–vis spectrophotometry.

Table 1
Comparison of the present method with other methods for pesticides determination.

Determination method	Measurement	Pesticide	LOD	Refs.
g-C_3N_4/$BiFeO_3$	Colorimetric	Carbaryl	0.033 μg/L	[42]
Dopant of acetone	Ion mobility spectrometer	Fenthion	0.07 mg/L	[43]
NiO-SPE	Electrochemical	Parathion	0.699 μg/L	[44]
AChE/Au NPs/Chi/GCE	Electrochemical	Carbaryl	1.408 μg/L	[45]
BSA-AuNCs/AChE	Fluorescence	Parathion-methyl	0.14 μg/L	[46]
SPAN/GCE	DPV	Parathion	0.436 μg/L	[47]
g-C_3N_4/AgNPs	Fluorescence/UV–vis	Parathion-methyl	0.0324 μg/L	This work

Table 2
Detection of PM spiked in real samples.

Sample	Added (μg/L)	Fluorescence			UV–vis		
($n = 3$)		Found (μg/L)	Recovery (%)	RSD (%)	Found (μg/L)	Recovery (%)	RSD (%)
Lake water	0	0	0	0	0	0	0
	0.1	0.12	120	3.5	0.12	120	3.1
	0.25	0.22	88	4.1	0.28	112	2.7
	0.5	0.59	118	2.6	0.46	92	3.7
Apple	0	0	0	0	0	0	0
	0.1	0.112	112	3.7	0.097	97	5.3
	0.25	0.265	106	2.4	0.198	79.2	2.5
	0.5	0.49	80	3.2	0.51	102	3.4
Carrot	0	0	0	0	0	0	0
	0.1	0.105	105	3.1	0.092	92	4.8
	0.25	0.19	76	4.2	0.253	101	3.1
	0.5	0.53	106	1.6	0.487	97.4	2.4

3.6. Dual-signal assay detection of PM

Under the optimal experimental conditions, PM was used as a target analyte using the double reading method. Fig. 7A shows the relationship between the PM concentration and the fluorescence intensity over a range of 0.1–1.0 μg/L. It can be expressed as follows: $y = -325.719x + 565.84$ ($R^2 = 0.991$) and the limit of detection (LOD) was 0.0324 μg/L. It can be seen from Fig. 7B that the absorbance of the AgNPs increased with an increasing concentration of PM at 390 nm, and an excellent linear relationship between the absorbance and the PM concentration over the range of 0.1–1.0 μg/L was observed. The calibration equation can be expressed as $y = 0.6323x + 0.56313$ (R^2=0.990) and the LOD was 0.056 μg/L. In addition, a comparison between our work and various other reported methods of analysis [42–47] is shown in Table 1, indicating that our method can achieve relatively high sensitivity and has a low detection limit.

3.7. Analysis of PM in real samples

To evaluate the feasibility of the use of the double reading method for real samples, a series of different concentrations of PM in water, apple, and carrot samples was analyzed. The results are shown in Table 2. The results indicated that the percentage of recovery from both spectral methods was in the range of 76%–120% and the relative standard deviation (RSD, $n = 3$) values were found to be <5.3%. These experimental results indicated that the nanoprobe for the detection of PM has a great practical value in food and environmental applications.

4. Conclusion

We have constructed an environmentally friendly and sensitive dual-signal nanoprobe (using UV–vis and fluorescence assays) based on g-C_3N_4/AgNPs to detect organophosphorus pesticides. The mechanism of the experimental method was confirmed by a series of characterizations using TEM images, the fluorescence spectrum, UV–vis absorption spectroscopy, fluorescence lifetime measurements, and zeta potential measurements, and the method was successfully applied to pesticide residue detection in real samples.

Declaration of competing interest

The authors declare that there are no conflicts of interest.

Acknowledgments

This work was financially supported by the National Natural Science Foundation of China (Grant No. 21765015, 21808099 to P. Qiu, 31860263 to X. Wang) and the Science and Technology Innovation Platform of Jiangxi Province (Grant No. 20192BCD40001), China.

References

[1] M. Eddleston, F. Worek, P. Eyer, et al., Poisoning with the S-Alkyl organophosphorus insecticides profenofos and prothiofos, QJM-Int. J. Med. 102 (2009) 785–792.
[2] M. Tankiewicz, J. Fenik, M. Biziuk, Determination of organophosphorus and organonitrogen pesticides in water samples, TrAC Trends Anal. Chem 29 (2010) 1050–1063.
[3] S. Qian, H. Lin, Colorimetric sensor array for detection and identification of organophosphorus and carbamate pesticides, Anal. Chem. 87 (2015) 5395–5400.
[4] S. Liao, W. Han, H. Ding, et al., Modulated dye retention for the signal-on fluorometric determination of acetylcholinesterase inhibitor, Anal. Chem. 85 (2013) 4968–4973.
[5] C.S. Pundir, N. Chauhan, Acetylcholinesterase inhibition-based biosensors for pesticide determination: a review, Anal. Biochem. 429 (2012) 19–31.
[6] M. Kushwaha, S. Verma, S. Chatterjee, Profenofos, an acetylcholinesterase-inhibiting organophosphorus pesticide: a short review of its usage, toxicity, and biodegradation, J. Environ. Qual. 45 (2016) 1478–1489.
[7] M. Liang, K. Fan, Y. Pan, et al., Fe_3O_4 magnetic nanoparticle peroxidase mimetic-based colorimetric assay for the rapid detection of organophosphorus pesticide and nerve agent, Anal. Chem. 85 (2013) 308–312.
[8] J.P. Ma, R.H. Xiao, H. Zhao, , et al.Benzhang Shi, Shuqing Li, Determination of organophosphorus pesticides in underground water by SPE-GC–MS, J. Chromatogr. Sci. 47 (2009) 110–115.
[9] B. Bucur, F.D. Munteanu, J.L. Marty, et al., Advances in enzyme-based biosensors for pesticide detection, Biosensors 8 (2018), 27.
[10] M. LeDoux, Analytical methods applied to the determination of pesticide residues in foods of animal origin. A review of the past two decades, J. Chromatogr. A 1218 (2011) 1021–1036.
[11] L. Zhang, Z. Wang, Y. Wen, et al., Simultaneous detection of parathion and imidacloprid using broad-specificity polyclonal antibody in enzyme-linked immunosorbent assay, Anal. Methods 7 (2015) 205–210.
[12] S. Zhang, X. Li, M. Zong, et al., A sensitive chemiluminescence enzyme immunoassay based on molecularly imprinted polymers solid-phase extraction of parathion, Anal. Biochem. 530 (2017) 87–93.
[13] M. Garcés-García, E.M. Brun, R. Puchades, et al., Immunochemical determination of four organophosphorus insecticide residues in olive oil using a rapid extraction process, Anal. Chim. Acta 556 (2006) 347–354.
[14] L. Tan, M. Guo, J. Tan, et al., Development of high-luminescence perovskite quantum dots coated with molecularly imprinted polymers for pesticide detection by slowly hydrolysing the organosilicon monomers in situ, Sens. Actuators B Chem. 291 (2019) 226–234.
[15] A.L. Jenkins, R. Yin, J.L. Jensen, Molecularly imprinted polymer sensors for pesticide and insecticide detection in water, Analyst 126 (2001) 798–802.
[16] J. Chen, X. Wei, H. Tang, et al., Highly discriminative fluorometric sensor based on luminescent covalent organic nanospheres for tyrosinase activity monitoring and inhibitor screening, Sens. Actuators B Chem. 305 (2020), 127386.
[17] Q. Long, H. Li, Y. Zhang, et al., Upconversion nanoparticle-based fluorescence resonance energy transfer assay for organophosphorus pesticides, Biosens. Bioelectron. 68 (2015) 168–174.
[18] S. Wang, X. Wang, X. Chen, et al., A novel upconversion luminescence turn-on nanosensor for ratiometric detection of organophosphorus pesticides, RSC

Adv. 6 (2016) 46317–46324.
[19] Y. Yi, G. Zhu, C. Liu, et al., A label-free silicon quantum dots-based photoluminescence sensor for ultrasensitive detection of pesticides, Anal. Chem. 85 (2013) 11464–11470.
[20] X. Gao, G. Tang, X. Su, Optical detection of organophosphorus compounds based on Mn-doped ZnSe-dot enzymatic catalytic sensor, Biosens. Bioelectron. 36 (2012) 75–80.
[21] Y. Yan, J. Sun, K. Zhang, et al., Visualizing gaseous nitrogen dioxide by ratiometric fluorescence of carbon nanodots-quantum dots hybrid, Anal. Chem. 87 (2015) 2087–2093.
[22] D. Liu, W. Chen, J. Wei, et al., A highly sensitive, dual-readout assay based on gold nanoparticles for organophosphorus and carbamate pesticides, Anal. Chem. 84 (2012) 4185–4191.
[23] M. Arvand, A.A. Mirroshandel, An efficient fluorescence resonance energy transfer system from quantum dots to graphene oxide nano sheets: application in a photoluminescence aptasensing probe for the sensitive detection of diazinon, Food Chem. 280 (2019) 115–122.
[24] Y. Zhan, J. Yang, L. Guo, et al., Targets regulated formation of boron nitride quantum dots – gold nanoparticles nanocomposites for ultrasensitive detection of acetylcholinesterase activity and its inhibitors, Sens. Actuators B Chem. 279 (2019) 61–68.
[25] Y. Gong, M. Li, Y. Wang, Carbon nitride in energy conversion and storage: recent advances and future prospects, ChemSusChem 8 (2015) 931–946.
[26] X.L. Zhang, C. Zheng, S.S. Guo, et al., Turn-on fluorescence sensor for intracellular imaging of glutathione using g-C_3N_4 nanosheet-MnO_2 sandwich nanocomposite, Anal. Chem. 86 (2014) 3426–3434.
[27] E.Z. Lee, S.U. Lee, N.S. Heo, , et al.W.H. Hong, A fluorescent sensor for selective detection of cyanide using mesoporous graphitic carbon(IV) nitride, Chem. Commun. 48 (2012) 3942–3944.
[28] G. Zhang, J. Zhang, M. Zhang, et al., Polycondensation of thiourea into carbon nitride semiconductors as visible light photocatalysts, J. Mater. Chem. 22 (2012) 8083–8091.
[29] Y. Cui, J. Zhang, G. Zhang, et al., Synthesis of bulk and nanoporous carbon nitride polymers from ammonium thiocyanate for photocatalytic hydrogen evolution, J. Mater. Chem. 21 (2011) 13032–13039.
[30] J. Tian, Q. Liu, A.M. Asiri, et al., Ultrathin graphitic carbon nitride nanosheets: a novel peroxidase mimetic, Fe doping-mediated catalytic performance enhancement and application to rapid, highly sensitive optical detection of glucose, Nanoscale 5 (2013) 11604–11609.
[31] N. Zhang, J. Gao, C. Huang, et al., In situ hydrothermal growth of ZnO/g-C_3N_4 nanoflowers coated solid-phase microextraction fibers coupled with GC-MS for determination of pesticides residues, Anal. Chim. Acta 934 (2016) 122–131.
[32] H. Yin, W. Jiang, P. Liu, et al., Photoelectrochemical immunosensing platform for *M. SssI* methyltransferase activity analysis and inhibitor screening based on g-C_3N_4 and CdS quantum dots, Sens. Actuators B Chem. 244 (2017) 458–465.
[33] X. Zhang, X. Xie, H. Wang, et al., Enhanced photoresponsive ultrathin graphitic-phase C_3N_4 nanosheets for bioimaging, J. Am. Chem. Soc. 135 (2013) 18–21.
[34] Q.J. Luo, Y.X. Li, M.Q. Zhang, et al., A highly sensitive, dual-signal assay based on rhodamine B covered silver nanoparticles for carbamate pesticides, Chin. Chem. Lett. 28 (2017) 345–349.
[35] J.R. Bhamore, P. Ganguly, S.K. Kailasa, Molecular assembly of 3-mercaptopropinonic acid and guanidine acetic acid on silver nanoparticles for selective colorimetric detection of triazophos in water and food samples, Sens. Actuators B Chem. 233 (2016) 486–495.
[36] Y. Wang, F. Yang, X. Yang, Colorimetric detection of mercury(II) ion using unmodified silver nanoparticles and mercury-specific oligonucleotides, ACS Appl. Mater. Interfaces 2 (2010) 339–342.
[37] D.G. Thompson, R.W. Stokes, R.W. Martin, et al., Synthesis of unique nanostructures with novel optical properties using oligonucleotide mixed–metal nanoparticle conjugates, Small 4 (2008) 1054–1057.
[38] H. Xie, F. Bei, J. Hou, et al., A highly sensitive dual-signaling assay via inner filter effect between g-C_3N_4 and gold nanoparticles for organophosphorus pesticides, Sens. Actuators B Chem. 255 (2018) 2232–2239.
[39] F. Xu, X. Jiang, J. Hu, et al., Nano g-C_3N_4/TiO_2 composite: a highly efficient photocatalyst for selenium (VI) photochemical vapor generation for its ultrasensitive AFS determination, Microchem. J. 135 (2017) 158–162.
[40] M. Zheng, Z. Xie, D. Qu, et al., On-off-on fluorescent carbon dot nanosensor for recognition of chromium(VI) and ascorbic acid based on the inner filter effect, ACS Appl. Mater. Interfaces 5 (2013) 13242–13247.
[41] X. Zhu, Y. Xiao, X. Jiang, et al., A ratiometric nanosensor based on conjugated polyelectrolyte-stabilized AgNPs for ultrasensitive fluorescent and colorimetric sensing of melamine, Talanta 151 (2016) 68–74.
[42] H. Ouyang, X. Tu, Z. Fu, et al., Colorimetric and chemiluminescent dual-readout immunochromatographic assay for detection of pesticide residues utilizing g-C_3N_4/$BiFeO_3$ nanocomposites, Biosens. Bioelectron. 106 (2018) 43–49.
[43] S.M. ZakirHossain, R.E. Luckham, M.J. McFadden, et al., Reagentless bidirectional lateral flow bioactive paper sensors for detection of pesticides in beverage and food samples, Anal. Chem. 81 (2009) 9055–9064.
[44] M. Khairy, H.A. Ayoub, C.E. Banks, Non-enzymatic electrochemical platform for parathion pesticide sensing based on nanometer-sized nickel oxide modified screen-printed electrodes, Food Chem. 255 (2018) 104–111.
[45] Y. Li, Z. Gan, Y. Li, et al., Immobilization of acetylcholinesterase on one-dimensional gold nanoparticles for detection of organophosphorous insecticides, Sci. China Chem. 53 (2010) 820–825.
[46] Q.J. Luo, Z.G. Li, J.H. Lai, et al., An on-off-on gold nanocluster-based fluorescent probe for sensitive detection of organophosphorus pesticides, RSC Adv. 7 (2017) 55199–55205.
[47] N.Y. Sreedhar, M.S. Kumar, Voltammetric determination of parathion at sulphonated polyaniline based electrochemical sensor, Anal. Bioanal. Electrochem. 5 (2013) 635–646.